Journal Pre-proof

Analysis of malaria infection byproducts with Mueller matrix transmission ellipsometry

P. Basa , B. Fodor , Zs. Nagy , B. Oyunbolor , A. Hajtman , S. Bordács , I. Kézsmárki , A. Halbritter , Á Orbán

PII: S0040-6090(22)00539-9
DOI: https://doi.org/10.1016/j.tsf.2022.139637
Reference: TSF 139637

To appear in: *Thin Solid Films*

Received date: 30 August 2022
Revised date: 8 December 2022
Accepted date: 12 December 2022

Please cite this article as: P. Basa , B. Fodor , Zs. Nagy , B. Oyunbolor , A. Hajtman , S. Bordács , I. Kézsmárki , A. Halbritter , Á Orbán , Analysis of malaria infection byproducts with Mueller matrix transmission ellipsometry, *Thin Solid Films* (2022), doi: https://doi.org/10.1016/j.tsf.2022.139637

This is a PDF file of an article that has undergone enhancements after acceptance, such as the addition of a cover page and metadata, and formatting for readability, but it is not yet the definitive version of record. This version will undergo additional copyediting, typesetting and review before it is published in its final form, but we are providing this version to give early visibility of the article. Please note that, during the production process, errors may be discovered which could affect the content, and all legal disclaimers that apply to the journal pertain.

© 2022 Published by Elsevier B.V.

Highlights

- Synthetic hemozoin suspensions were studied by Mueller matrix transmission ellipsometry
- Hemozoin crystals were oriented by external magnetic field, while the sample was measured by ellipsometer
- Magnetic field rotation induced changes in Mueller matrix spectrum
- Hemozoin concentration can be calculated based on the presented analysis

Journal Pre-proof

Analysis of malaria infection byproducts with Mueller matrix transmission ellipsometry

P. Basa[1], B. Fodor[1], Zs. Nagy[1], B. Oyunbolor[1], A. Hajtman[1], S. Bordács[2], I. Kézsmárki[2,3], A. Halbritter[2], Á Orbán[2]

[1]*Semilab Co. Ltd., 1117 Budapest, Prielle K. u. 4/A, Hungary*
[2]*Department of Physics, Budapest University of Technology and Economics, 1111 Budapest, Budafoki út 8., Hungary*
[3]*Experimental Physics V, Center for Electronic Correlations and Magnetism, University of Augsburg, 86159 Augsburg, Universitätsstraße 1, Germany*

Abstract

In this work, hemozoin, a microcrystalline byproduct of the malaria parasites was studied by transmission Mueller matrix ellipsometry. Measurement data was collected for different magnetic field orientations and as a function of the density of the hemozoin suspension. Our ellipsometric study demonstrates the magnetic alignment of the hemozoin crystals via the corresponding large linear birefringence and dichroism signals. These results reveal optical anisotropies of this material, which could be utilized for future optimization of detection schemes or optical instruments for diagnostic use.

Introduction

Malaria is putting nearly half of human population at risk being a deadly and highly infectious tropical disease [1]. The cause of this illness is the *Plasmodium* parasite, which is being spread by mosquitoes infecting human blood [2]. The presence of the infection can be identified by conventional methods such as optical microscopy, rapid diagnostic tests and polymerase chain reaction [3-5]. A simple magneto-optical polarimeter-based setup was proposed recently, capable of even field-testing patients based on empirical polarization characteristics of the examined specimen [6]. The physical principle behind the detection is based on the anisotropic optical and magnetic properties of hemozoin, a microcrystalline byproduct of the malaria parasites, that can be co-aligned via moderate external magnetic fields due to its anisotropic paramagnetic susceptibility [7, 8]. In the field, the suspension of co-aligned needle-like hemozoin crystals becomes optically anisotropic, which is detected by a polarization-sensitive optical setup in the aforementioned detection method [9]. The detailed understanding of the optical anisotropies of the hemozoin suspension allowing for magneto-optical detection of malaria infection, are still not yet explored in the literature. Mueller matrix ellipsometry is widely used recently for the characterization of anisotropic media [10-13]. In this work, we propose transmission Mueller matrix spectroscopic ellipsometry to measure the hemozoin suspension response to external magnetic fields.

Experimental details

Synthetic hemozoin crystals [14] suspended in water were prepared in two different target concentrations. The actual resulted concentrations were verified by reference method [9] and were found to be ~1400 (au) for sample C1, and ~7200 (au) for sample C2. Please, note, that these concentrations are approximately 2 to 3 orders of magnitude higher than the ones obtained on typical real-life malaria infected blood samples [6]. These two samples were investigated both in the absence and presence of magnetic field, using spectroscopic ellipsometry. To generate an external magnetic field, a rotatable, cylindrical hollow Halbach-magnet was used with nominal strength of ~1 T. The spectroscopic ellipsometer, a Semilab SE-2000 was used in straight-line arrangement with double rotating compensator to measure the normalized 15-element Mueller matrix (M). Normalization is performed with the first element of M (m_{11}). The measurement setup is shown in Fig. 1., with the photo of the actual apparatus shown in insert (a). The Halbach-magnet was either rotated to (i) 0° or 90° azimuth orientations, i.e., „p" and „s" directions in the usual nomenclature (as shown in Fig. 1. insert b); (ii) rotated in between 0-360° by steps of 22.5°; or (iii) completely removed and substituted by a non-magnetic aluminium-made „dummy" object, keeping the sample in the same geometrical location as it was with the magnet.

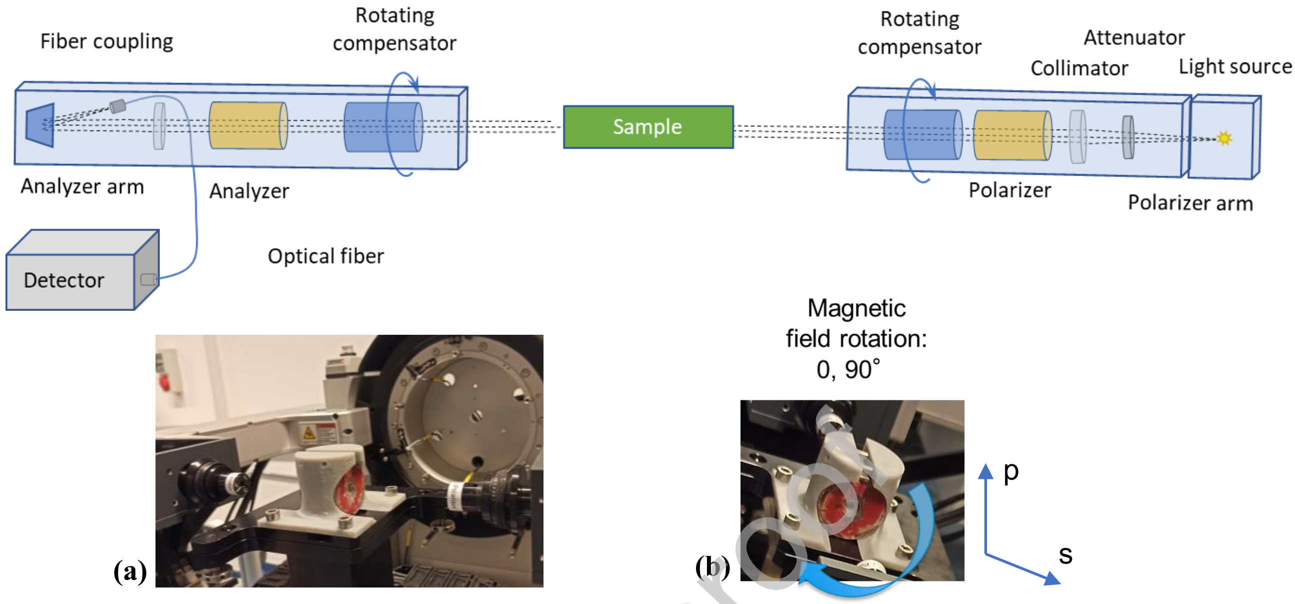

Fig. 1.: Measurement setup for collecting the normalized 15-element Mueller matrix. Insert (a): photo of the actual apparatus, Insert (b): illustration of the magnetic rotation direction.

Theory/calculation

Mueller matrix decomposition

A Lu-Chipman type Mueller matrix decomposition based on the work of Ping et al. [15] was used in a step-by-step approach as illustrated in Fig. 2. Mueller matrix decomposition provides separation of depolarization and window strain from the various birefringence and dichroism of the sample. After performing a series of measurements sequentially to separate the individual contributions of each component in the measurement system, Eqs. 1-2 were used as a basis for our regression algorithm to calculate the rotation parameters: the magnet orientation, the cuvette orientation, and we also fitted the hemozoin concentration ratio. The following protocol was applied in each series of measurements: first, the free-air baseline is measured noted as M_B (Fig. 2a.) to verify the self-consistency of the ellipsometer measurement system, i.e., to obtain a baseline correction. As a second step, the sample was measured without any external magnetic field (Fig. 2b.). This provided a reference M, termed: M_R, which was used to deduce the contribution of the cuvette orientation by determining its polarization rotation and the window strain. The related equation is shown in in Fig. 2b, with notation M_R^{Δ} for contribution originating from depolarization, M_R^{R} for retardance, M_R^{D} for diattenuation, M_R^{C} for circular retardance, and M_R^{W} for window strain. Finally, as a third step, the Mueller matrix with the sample placed in an external magnetic field orienting the hemozoin crystals was measured, termed: M_S' (Fig. 2c.).

Journal Pre-proof

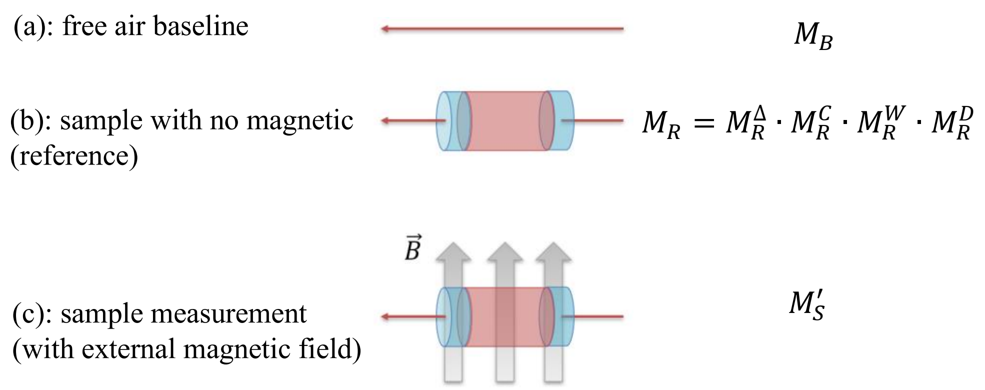

Fig. 2.: Sequence of measurements for the calculation of the individual contributions to the measured signal

By performing this sequence of measurements, the original Mueller matrix contribution of the sample, M_S can be obtained by using Eq. 1.

$$M_S = M_R^{-1} \cdot M_S' \qquad \textit{Eq. 1.}$$

The regression model

By expanding the contributions, one can obtain Eq. 2., where angles α_m and α_c describes the orientations of the field-aligned hemozoin microcrystals and the cuvette with respect to the “p” (vertical) polarization direction of the setup and c, the concentration of the hemozoin. We determined these variables by numerical regression where a composed M based on the decomposed matrices of the reference measurements are directly compared to the results of the measurements performed on the hemozoin suspensions in magnetic field. Here, contribution from the rotated cuvette is grouped in ⌊ ⌋ brackets, and contribution from the sample in rotated magnetic field is grouped in ⌈ ⌉ brackets.

$$M_S'^{meas} \leftrightarrow M_S'^{calc} = M_R^{\Delta} \cdot M_R^{C} \cdot \lfloor R(-\alpha_c) \cdot M_R^{W} \cdot R(\alpha_c) \rfloor \cdot \lceil R(-\alpha_m) \cdot M_S^{R}(c) \cdot M_S^{D}(c) \cdot R(\alpha_m) \rceil \qquad \textit{Eq. 2}$$

The ↔ symbol indicates that the measured M_S' on the left is fitted via numerical regression with the model decomposition on the right.

The numerical regression solves a least squares problem, and compares the measured Mueller matrix elements to calculated Muller matrix elements, and the S sum of squared residuals is minimized over the variable space (c, α_m, α_c) to find the optimal variables.

$$S = \sum_{ij} \sum_{\lambda} \left[(m_S')_{ij\,\lambda}^{calc}(c, \alpha_m, \alpha_c) - (m_S')_{ij\,\lambda}^{meas} \right]^2 \qquad \textit{Eq. 3.}$$

where i and j are the index of the Mueller matrix elements from 1 to 4, and λ is indexing the data points for the different wavelengths. The actual numerical method used for this problem is a Quasi-Newton with BFGS (Broyden–Fletcher–Goldfarb–Shanno) algorithm.

Extracting window strain from measurement data

The window strain is modeled by a rotated retarder

$$M_R^{W}(w, \delta_w) = R(-w) \cdot C(\delta_w) \cdot R(w) \qquad \textit{Eq.4.}$$

where R is a rotation matrix, and C is the Mueller matrix of an ideal retarder (compensator), while w is the rotation angle and δ_w is the phase shift of the retarder. This single expression describes both windows together, with an effective w and δ_w. Normally we should treat the two windows of the cuvette separately. However, the strain is small, therefor the $M_R^{W}(w,\delta_w)$ matrix is close to the unit matrix, and becomes approximately commutative with M_S, the Mueller matrix of the sample.

Expanding equation provides Mueller matrix elements of $M_R^{W}(w,\delta_w)$

Journal Pre-proof

$$m_{24} = -sin\,(\delta_w) \cdot sin\,(2w) \qquad \textit{Eq. 5.}$$

$$m_{34} = sin\,(\delta_w) \cdot cos\,(2w) \qquad \textit{Eq. 6.}$$

$$m_{44} = cos\,(\delta_w) \qquad \textit{Eq. 7.}$$

Because δ_w is small, it is better not to use m_{44}, errors would be too high. Only m_{24} and m_{34} are used to determine δ_w and w. As w is independent on wavelength, while M elements are wavelength dependent, w is calculated by averaging over the whole wavelength range.

$$w = \frac{1}{n}\sum_{\lambda=1}^{n}\frac{1}{2}atan\left(\frac{-m_{24}(\lambda)}{m_{34}(\lambda)}\right) \qquad \textit{Eq.8.}$$

while δ_w can be calculated by

$$\delta_w(\lambda) = \frac{1}{2}\sqrt{m_{24}(\lambda)^2 + m_{34}(\lambda)^2} \qquad \textit{Eq. 9.}$$

The results fit fine on a low strain glass model, where the strain induced phase shift can be calculated as

$$\delta_w = \Delta n \cdot d/\lambda \cdot 2\pi \qquad \textit{Eq. 10.}$$

where Δn is the birefringence of the glass and d is the window thickness.

Extracting birefringence and dichroism of hemozoin from measurement data

M_R^{Δ}, M_R^{C} and M_R^{W} are calculated from the reference measurement [15], and the Mueller matrix of the sample can be calculated according to Eq.1 and Eq.2

$$M_S = (M_R^{\Delta})^{-1} \cdot (M_R^{C})^{-1} \cdot (M_R^{W})^{-1} \cdot M_S' \qquad \textit{Eq. 11.}$$

Then M_S is decomposed to depolarization, diattenuation and retardance, M_S^{Δ}, M_S^{D} and M_S^{R} respectively.

We determine the birefringence of the hemozoin from M_S^{R} using the same rotated retarder model described above, with the only difference that the rotation angle, w is replaced by the magnetic orientation, α_m. We obtained the retardance, δ_H differently as it changes sign over the wavelength range. Birefringence of the hemozoin is $HB = \sin\delta_H$.

$$HB = sin\delta_H = \frac{(m_S^R)_{24}}{-\,sin\,\alpha_m} \qquad \textit{Eq. 12.}$$

α_m is calculated first, then the hemozoin birefringence is calculated from a measurement, where $\sin\alpha_m$ is close to 1.

M_S^{D} contains hemozoin dichroism HD, and according to the decomposition model it can be extracted from the first column (diattenuation vector) of the Mueller matrix M_S^{D}

$$HD = cos2\psi_H = \sqrt{{(m_S^D)_{21}}^2 + {(m_S^D)_{31}}^2} \qquad \textit{Eq. 13.}$$

The higher concentration sample (C2) was used to extract the birefringence and dichroism of the hemozoin, because the lower relative noise levels.

Hemozoin concentration in the regression model

The concentration is used as a linear scaling factor for both birefringence and dichroism.

$$M_S^R(c) = \begin{bmatrix} 1 & . & . & . \\ . & 1 & . & . \\ . & . & \sqrt{1-(c\cdot HB)^2} & c\cdot HB \\ . & . & -c\cdot HB & \sqrt{1-(c\cdot HB)^2} \end{bmatrix} \qquad \textit{Eq. 14.}$$

while the M_S^{D} (c) matrix is calculated based on the decomposition method described in ref. [15], using D=[-c·HD, 0, 0] diattenuation vector.

Journal Pre-proof

The same c concentration was used for calculating M_S^R (c) and M_S^D (c), and also the same α_m magnet direction for the rotation matrices. It was supposed that the depolarization is negligible, which is in good agreement with the measurement data. The concentration dependent Mueller matrix of the sample can be calculated as

$$M_S(c)=R(-\alpha_m) \cdot M_S^R(c) \cdot M_S^D(c) \cdot R(\alpha_m) \quad \text{Eq. 15.}$$

The used linear model is a simplification for the two different samples to be used for evaluations. These two data points only shows that an approximately linear expression can describe the concentration dependance for both birefringence and dichroism. On one hand it is clear, that higher concentration will bring in nonlinear effects, and the current linear model cannot describe the concentration dependance properly. But on the other hand, any real infected blood samples contain hemozoin in (much) lower concentration, than our two synthetic samples, therefor the assumed linear concentration dependence is adequate for a wide concentration range, including all of the biological samples.

Results and Discussion

Fig. 3 shows the measured 15-element normalized transmission Mueller matrix(*M*), as recorded by either with or without the magnet providing an external magnetic field to the hemozoin suspension sample (C2). Without the magnet, the *M* spectrum is in good agreement with the expectations namely the *M* is close to the unity matrix with small perturbations from the window birefringence. By placing the magnet in the setup, however, some elements of the matrix significantly change, most notably: m_{12}, m_{21}, m_{13}, m_{31}, m_{34}, m_{43}, and m_{24}, m_{42}.

According to J. Freudenthal, [16], most anisotropic samples in transmission show only linear extinction (*LE*) and linear retardance (*LR*), which are basically the magnetic field induced linear dichroism and linear birefringence, respectively:

$$LE = k_p - k_s \quad \text{Eq. 16.}$$

$$LR = Phase(T_p) - Phase(T_s) \quad \text{Eq. 17.}$$

where T_p(T_s) and k_p(k_s) are the transmission and extinction coefficients for p(s) polarization, respectively. In case of phase, only orientation parallel to the molecular axis represents absorption, k component in the other direction is 0. These provide significant contribution to elements m_{12}, m_{21}, and m_{13}, m_{31} originating from *LE*, and m_{34}, m_{43}, and m_{24}, m_{42} originating from *LR*.

Journal Pre-proof

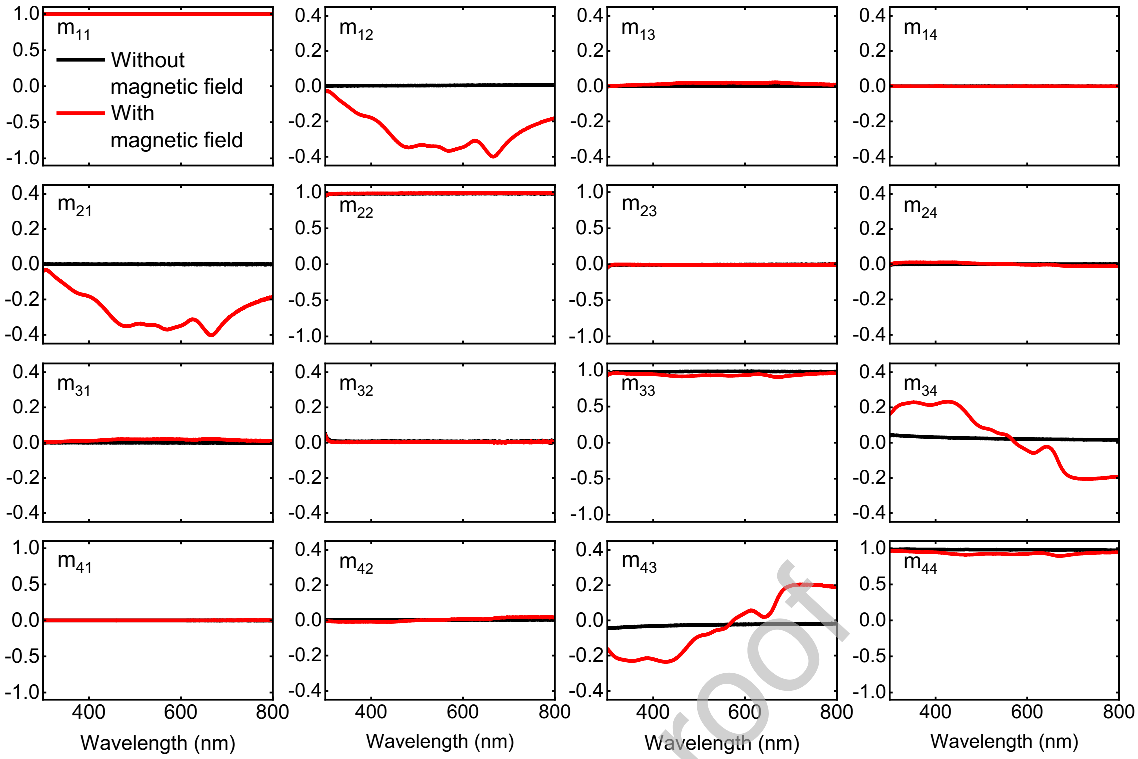

Fig. 3.: 15-element normalized Mueller matrix of sample C2 without (black) and with (red) external magnetic field (~1 T) oriented at 0°

This explanation is further supported by the experimental results, when the magnetic field is rotated by 90°, i.e., the orientation of the hemozoin microcrystals is rotating with respect to p and s directions. In this case, the p and s components are reversed in Eq. 16, which results in a sign change in m_{12} and m_{21}. As described above, the phase of either p or s directions is zero due to orthogonality. Therefore, Mueller matrix elements m_{34} and m_{43} should also change sign, which is in agreement with our results shown in Fig. 4.

The M spectra measured at several magnetic field directions in between 0-360° with steps of 22.5° are shown in Fig. 4a and b for samples C1 and C2, respectively. Increase in hemozoin concentration from sample C1 to C2 leads to increased amplitude of the significant Mueller matrix elements, which is proportional to the change in the concentration (5.14 times increase from sample C1 to C2).

Journal Pre-proof

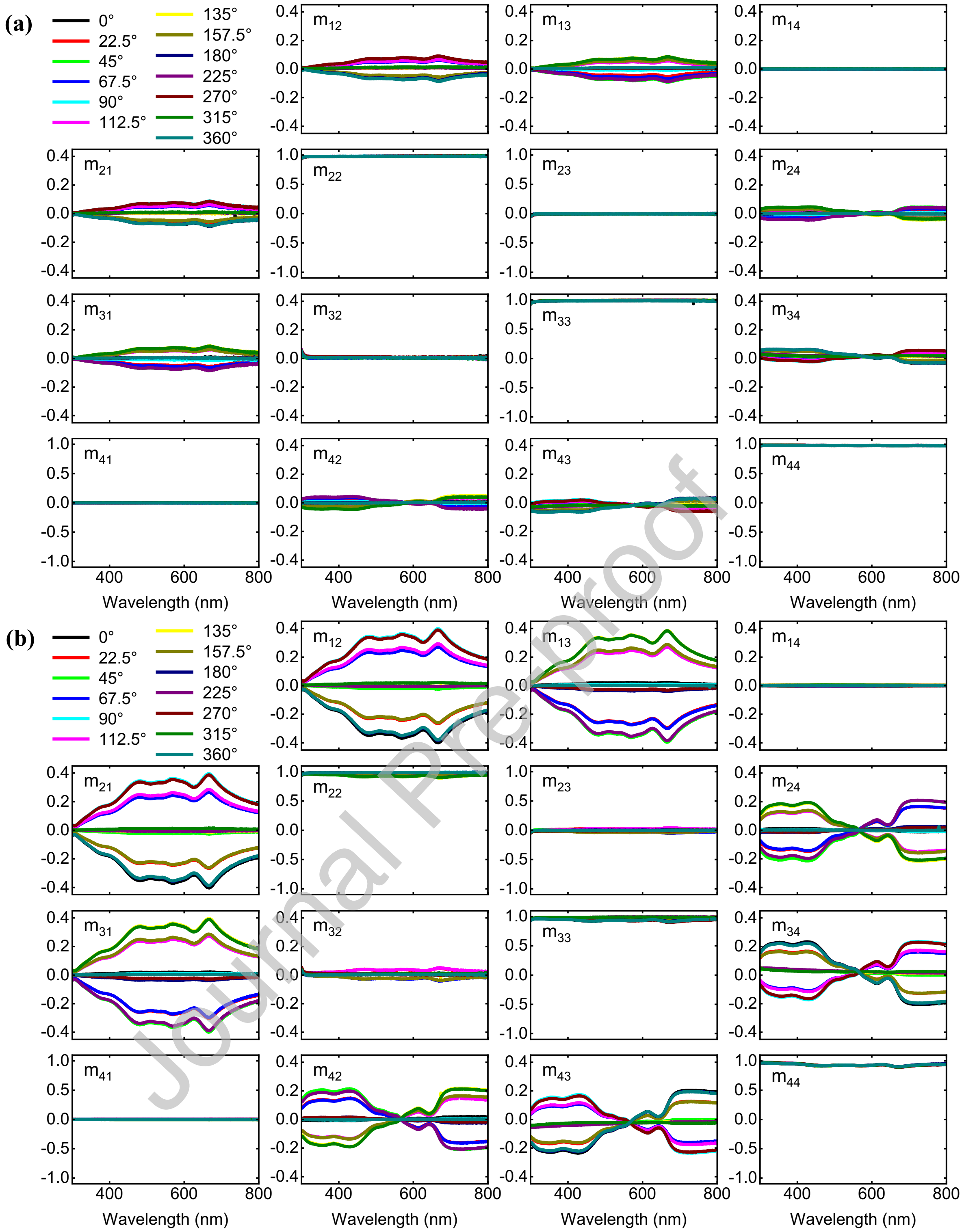

Fig. 4.: 15-element normalized Mueller matrix elements of the sample with magnetic excitation rotation in between 0-360° with steps of 22.5° for sample C1 and C2 shown in a and b panels, respectively

Decomposed M elements are shown for the reference measurement in Fig. 5a. It was found that depolarization, linear and circular dichroism are negligible, however, retardance seems significant in elements m_{34} and m_{43}. This is typical in case of a glass window with finite birefringence, and it can be subtracted as a reference from measurements with the sample.

Journal Pre-proof

Fig. 5b. shows the decomposition of the measured Mueller matrix for the C2 sample at 270° magnet orientation. Both retardance and diattenuation elements are significant, while depolarization is similarly negligible, just like in case of the reference measurement. In case of exactly 270° magnet orientation, some elements, like m_{13} should be exactly zero, while m_{24} should only show cuvette retardance, and no sample retardance. However, these elements are affected by the hemozoin sample. Regression shows that the magnet orientation was actually 267.7° instead of the targeted 270°, and the rotation matrix will mix the rows 2 and 3, also the columns 2 and 3. Therefor hemozoin spectra appears in m_{13} and m_{24} Mueller matrix elements with small amplitude.

Journal Pre-proof

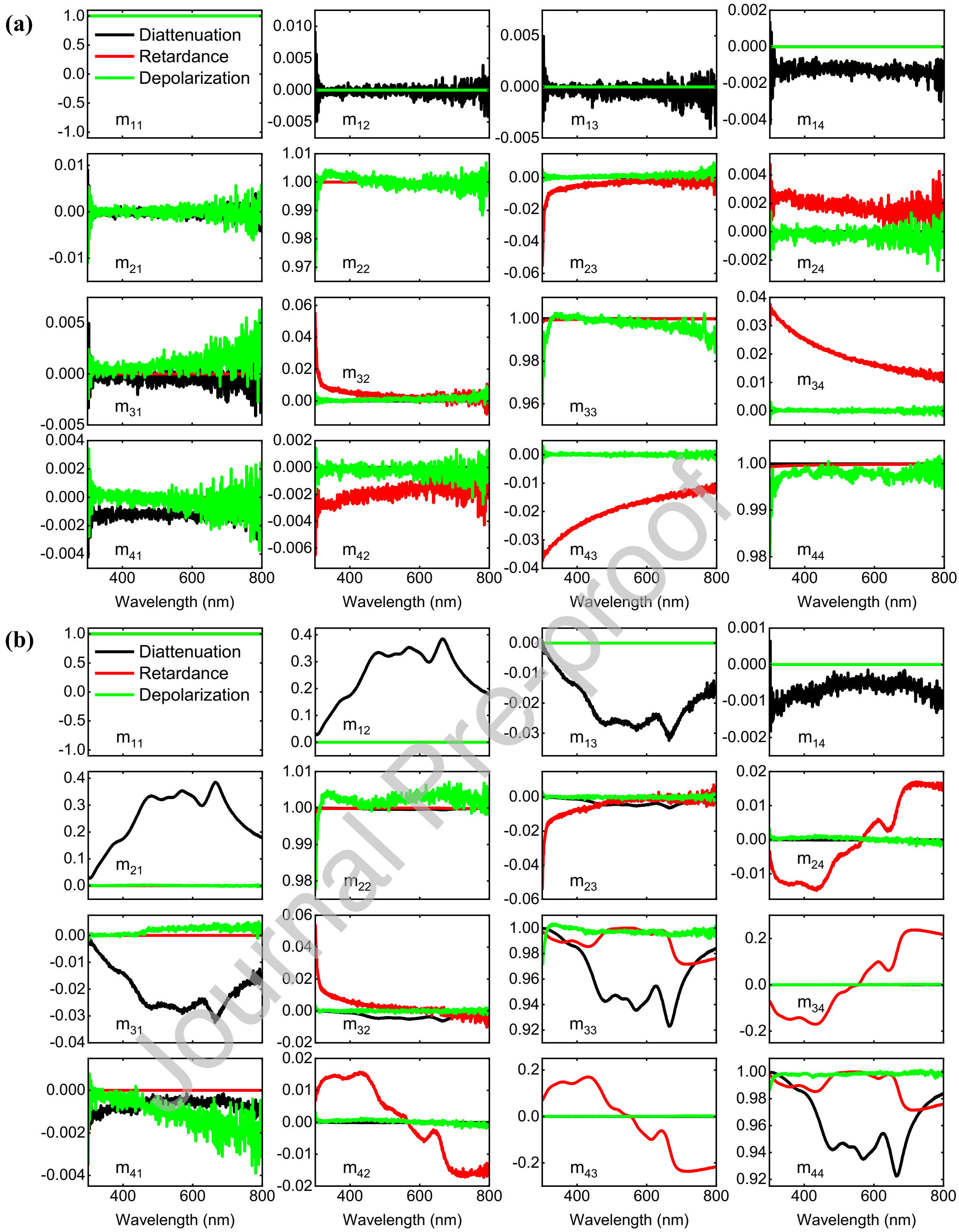

Journal Pre-proof

Fig. 5.: a) Decomposed Mueller matrix of a reference measurement (M_R). b) Decomposed Mueller matrix of the C2 sample measurement (M_S') with magnet oriented at 270° direction. Curves are black for diattenuation, red for retardance, and green for depolarization

Numerical regression on measurements with each magnetic field angle was performed based on the method described above. Typical fits of the measurements on samples C1 and C2 are shown in Fig. 6. at 270° field rotation angle (with respect to the "p", vertical direction). Acceptable noise level of the measurements was found, that was typically in the order of <0.001 for each *M* elements, and regression error was found to be also acceptable, in the range of <0.005, respectively.

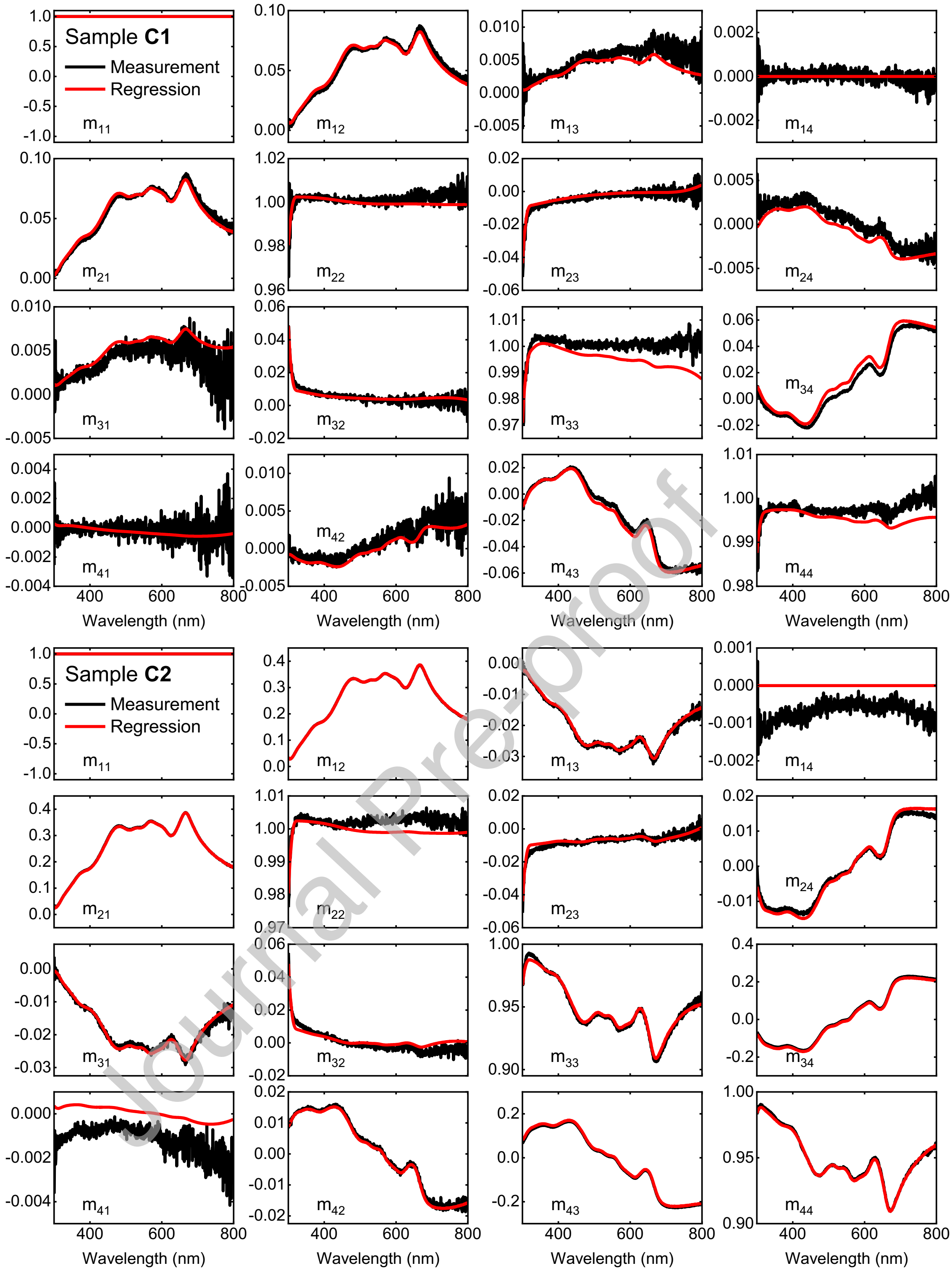

Fig. 6.: Typical fit result on a sample measurement: C1 and C2 at 270° magnetic rotation

Fit result for magnetic field orientation angle shows excellent agreement with experimental settings both for sample C1 and C2, indicating self-consistency of the method (see Fig. 7).

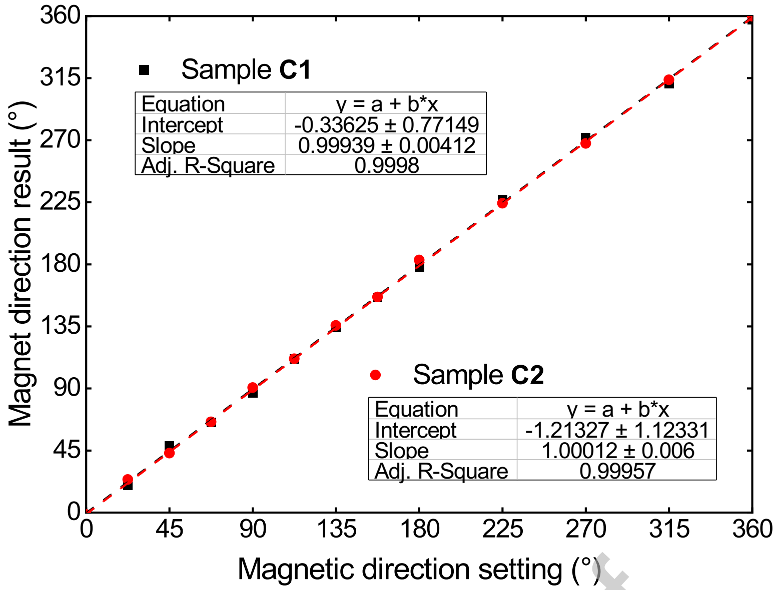

Fig. 7.: Fit result for magnetic field orientation angle vs. experimental setting for sample C1 (black squares) and C2 (red circles)

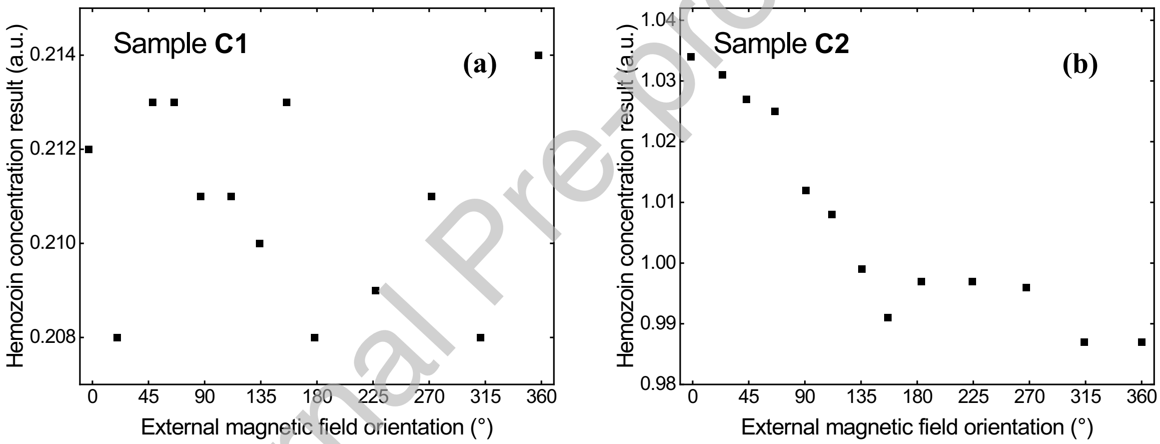

Fig. 8.: Fitted (normalized) Hemozoin concentration vs. magnet rotation (°) for sample C1 and C2, (figures a and b, respectively). Result suggests initial segregation/sedimentation effect vs. experiment time for sample C2

Journal Pre-proof

As the field is rotated with α_m, the m_{12} and m_{21} elements followed $\cos(2\alpha_m)$ angular dependence whereas the m_{13} and m_{31} components varied as $\sin(2\alpha_m)$. The amplitude of the angular dependence (or the average of the amplitudes for the different matrix elements) is proportional to the hemozoin concentration, which was plotted in Fig. 8 for both studied samples. As expected, the concentration, as a material property of the sample does not depend on the external field orientation. The ratio of the concentration of sample C1 and C2 calculated by numerical regression (~ 1:5) was in good agreement with the results of the reference method. In case of the higher concentration sample (C2), one can observe a slow, slight decrease of the measured quantity, as shown in Fig. 8b. This phenomenon can be attributed to a slow sedimentation and aggregation of the individual hemozoin crystallites during the course of the measurement sequence.

Conclusion

In conclusion, synthetic hemozoin suspensions were studied by Mueller matrix transmission ellipsometry. We demonstrated that hemozoin crystals are oriented by an external magnetic field as shown by the field-induced emergence of linear extinction and retardance in the raw *M* spectrum. The measured *M* was analysed in detail by Mueller matrix decomposition, and good consistency and agreement were found in terms of resulted quantities, such as magnetic field orientation or hemozoin concentration. We found that Mueller matrix transmission ellipsometry is capable to detect hemozoin and analyse its optical anisotropies, which makes this method applicable for the study of the optical anisotropies introduced or influenced by magnetic fields.

Declaration of interests

☒ The authors declare that they have no known competing financial interests or personal relationships that could have appeared to influence the work reported in this paper.

Credit author statement

P. Basa: Conceptualization, Writing–original draft, Visualization, Supervision, Project administration

Á Orbán: Investigation. Resources, Writing–review and editing, Methodology

B. Fodor: Investigation, Data curation, Methodology

Zs. Nagy: Methodology, Data curation, Formal analysis

B. Oyunbolor: Writing–review and editing

A. Hajtman: Resources

S. Bordács: Writing–review and editing

I. Kézsmárki: Funding acquisition

A. Halbritter: Funding acquisition

References

[1] WHO *World malaria report 2021*, ISBN 978-92-4-004049-6

[2] A. F. Cowman, J. Healer, D. Marapana and K. Marsh, *Malaria: Biology and Disease* Cell 167, 610 (2016).

[3] *Basic Malaria Microscopy*. Second edition.Geneva: World Health Organization. 2010.

[4] *Malaria rapid diagnostic test performance: results of WHO producttesting of malaria RDTs: round 7* (2015-2016). Geneva: World Health Organization. 2017.

[5] S. Britton, Q. Cheng and J. S. McCarthy, *Novel molecular diagnostictools for malaria elimination: a review of options from the point of view of high-throughput and applicability in resource limited settings*, Malar. J. 15, 88 (2016)

[6] L. Arndt, T. Koleala, Á. Orbán, C. Ibam, E. Lufele, L. Timinao, L. Lorry, Á. Butykai, P. Kaman, A.P. Molnár, and S. Krohns, *Magneto-optical diagnosis of symptomatic malaria in Papua New Guinea*, Nat. Commun. 12, 969 (2021). https://doi.org/10.1038/s41467-021-21110-w, and references therein.

[7] D. S. Bohle, P. Debrunner, P. A. Jordan, S. K. Madsen and C. E. Schulz, *Aggregated Heme Detoxification Byproducts in Malarial Trophozoites:β-Hematin and Malaria Pigment Have a Single S = 5/2 IronEnvironment in the Bulk Phase as Determined by EPR and Magnetic Mössbauer Spectroscopy*, J. Am. Chem. Soc. 120, 8255 (1998)

[8] M. Walczak, K. Lawniczak-Jablonska, A. Sienkiewicz, I.N. Demchenko, E. Piskorska, G. Chatain and D.S Bohle, *Local environment of iron in malarial pigment and its substitute β-hematinin*, Nucl. Instrum. Meth. B238, 32 (2005).

[9] A. Butykai, A. Orban, V. Kocsis, D. Szaller, S. Bordács, E. Tátrai-Szekeres, L. F. Kiss, A. Bóta, B. G. Vértessy, T. Zelles and I. Kézsmárki, *Malaria pigmentcrystals as magnetic micro-rotors: key for high-sensitivity diagnosis*, Sci Rep. 3, 1431 (2013).

[10] Z. Guo, H. Gu, M. Fang, L. Ye, and S. Liu, *Giant in-plane optical and electronic anisotropy of tellurene: a quantitative exploration. Nanoscale*, 14(34), pp.12238-12246 (2022).

[11] G.A. Ermolaev, D.V. Grudinin, Y.V.Stebunov, K.V. Voronin, V.G Kravets, J. Duan, A.B. Mazitov, G.I. Tselikov, A. Bylinkin, D.I. Yakubovsky, and S.M Novikov, *Giant optical anisotropy in transition metal dichalcogenides for next-generation photonics*, Nature communications, 12(1), pp.1-8 (2021).

Journal Pre-proof

[12] Z. Guo, H. Gu, M. Fang, B. Song, W. Wang, X. Chen, C. Zhang, H. Jiang, L. Wang, and S. Liu, 2021. *Complete dielectric tensor and giant optical anisotropy in quasi-one-dimensional ZrTe5*, ACS Materials Letters, 3(5), pp.525-534 (2021).

[13] S. Hou, Z. Guo, J. Yang, Y.Y Liu, W. Shen, C. Hu, S. Liu, H. Gu, and Z. Wei, *Birefringence and dichroism in quasi-1D transition metal trichalcogenides: direct experimental investigation*, Small, 17(21), p.2100457 (2021).

[14] A.F. Slater, W.J Swiggard, B.R. Orton, W.D. Flitter, D.E. Goldberg, A. Cerami and G.B. Henderson, *An iron-carboxylate bond links the heme units of malaria pigment*, Proc. Natl. Acad. Sci. U.S.A. 88, 325 (1991).

[15] P. Sun, Y. Ma, W. Liu, Q. Yang and Q. Jia, *Mueller matrix decomposition for determination of optical rotation of glucose molecules in turbid media*, J. of Biomedical Optics, 19(4), 046015 (2014), https://doi.org/10.1117/1.JBO.19.4.046015

[16] J. Freudenthal, "*Intuitive interpretation of Mueller matrices of transmission.*" White Paper of Hinds Instruments Inc., Hillsboro, OR, Tech. Rep (2018). https://www.hindsinstruments.com/knowledge-center/product-document-library/product-literature/

Journal Pre-proof